Chemical Engineering Journal 367 (2019) 304–313

Contents lists available at ScienceDirect

Chemical Engineering Journal

journal homepage: www.elsevier.com/locate/cej

Heterogeneous photocatalysis using UVA-LEDs for the removal of antibiotics and antibiotic resistant bacteria from urban wastewater treatment plant effluents

Francesco Biancullo[a,b], Nuno F.F. Moreira[a,c], Ana R. Ribeiro[a], Célia M. Manaia[d], Joaquim L. Faria[a], Olga C. Nunes[c], Sérgio M. Castro-Silva[b], Adrián M.T. Silva[a,*]

[a] Laboratory of Separation and Reaction Engineering – Laboratory of Catalysis and Materials (LSRE-LCM), Faculdade de Engenharia, Universidade do Porto, Rua Dr. Roberto Frias, 4200-465 Porto, Portugal
[b] Adventech-Advanced Environmental Technologies, Centro Empresarial e Tecnológico, Rua de Fundões 151, 3700-121 São João da Madeira, Portugal
[c] LEPABE – Laboratory for Process Engineering, Environment, Biotechnology and Energy, Faculdade de Engenharia, Universidade do Porto, Rua Dr. Roberto Frias, 4200-465 Porto, Portugal
[d] Universidade Católica Portuguesa, CBQF – Centro de Biotecnologia e Química Fina – Laboratório Associado, Escola Superior de Biotecnologia, Rua Arquiteto Lobão Vital, Apartado 2511, 4202-401 Porto, Portugal

HIGHLIGHTS

- Antibiotics, bacteria and ARB removal in secondary treated urban wastewater.
- Antibiotics are efficiently oxidized by TiO_2-photocatalysis with UVA-LEDs.
- Methanol has a scavenging effect on the removal of the antibiotics.
- Efficient inactivation of cultivable bacteria including those antibiotic resistant.
- Bacterial regrowth is observed after 3-days storage of treated wastewater.

GRAPHICAL ABSTRACT

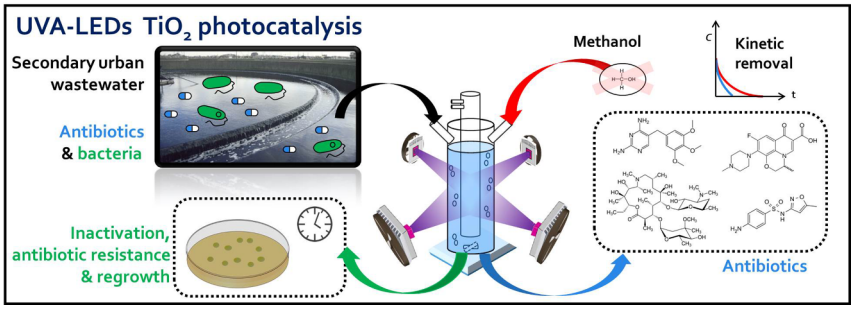

ARTICLE INFO

Keywords:
TiO_2-P25
Light emitting diodes (LEDs)
Micropollutant
Disinfection
Antibiotic resistant bacteria
Bacterial regrowth

ABSTRACT

Secondary urban wastewater samples were spiked with azithromycin (AZT), trimethoprim (TMP), ofloxacin (OFL) and sulfamethoxazole (SMX) at 100 $\mu g\,L^{-1}$ to investigate the efficiency of a TiO_2-photocatalytic treatment using UVA-LEDs. Different operating parameters were studied, such as the irradiation conditions, catalyst load and the use of methanol as carrier solvent and radical scavenger. The most efficient conditions to treat spiked urban wastewater (4 LEDs symmetrically distributed and 1.00 $g\,L^{-1}$ of catalyst) were also assessed on the removal of the antibiotics at real concentrations, as well as on the inactivation and regrowth of bacteria after 3-day storage (total and resistant heterotrophs, *Escherichia coli* and enterococci). Clindamycin (CLI) was targeted when SMX was not detected. One-hour treatment was enough to reduce the analysed antibiotics to values below the detection limits and to decrease the bacterial load by 2 log-units. Bacterial regrowth was observed for total heterotrophs, after the storage of photocatalytic treated wastewater, to values close to pre-treatment. However, the antibiotic resistance percentage of such stored wastewater was always similar or lower than that of secondary urban wastewater. Thus, the potential of this process as part of the tertiary treatment is demonstrated, but conditions must be adjusted to minimize microbial regrowth.

* Corresponding author.
E-mail address: adrian@fe.up.pt (A.M.T. Silva).

https://doi.org/10.1016/j.cej.2019.02.012
Received 15 November 2018; Received in revised form 30 January 2019; Accepted 2 February 2019
Available online 02 February 2019

1. Introduction

Antibiotics are frequently found at concentrations ranging from a few ng L^{-1} to μg L^{-1} in many aquatic compartments, namely wastewater influents and effluents, surface waters, groundwater and even in drinking water [1–3]. The use of this class of pharmaceuticals in human and veterinary medicine has triggered the introduction and accumulation of such compounds in the aquatic environment [4]. Given the potential adverse effects of these contaminants, the European Decisions 2015/495/EU and 2018/840/EU included azithromycin and other antibiotics in the Watch List of environmental concern, which should be monitored in surface waters [5,6].

Urban wastewater treatment plants (UWWTPs) are considered gateways of antibiotics into the aquatic environment and hot-spots for antibiotic resistance proliferation [7–9]. The presence of antibiotics, antibiotic resistant bacteria and antibiotic resistant genes (A&ARB&ARGs) in the environment, in particular throughout the urban water cycle and food chain, is considered a severe public health issue. In this regard, new approaches to reduce A&ARB&ARGs in water and to avoid the negative impacts on the downstream environment are necessary, in particular when the objective is to achieve good quality standards for possible reuse of urban wastewater (UWW) [10–12].

Ultraviolet (UV) irradiation is widely implemented as part of the tertiary treatment in UWWTPs [13,14]. Although the market offers a wide range of UV lamps, medium or low-pressure mercury vapour lamps emitting UVC light are preferred in UWW disinfection due to their germicidal power. Nonetheless, bacterial regrowth after water storage may disturb the original bacterial culture or favour ARB persistence [15–17]. Moreover, lab- and pilot-scale studies have demonstrated the inefficiency of UVC to remove different antibiotics from aqueous solutions [18,19]. Thus, oxidants and/or catalysts (e.g., H_2O_2, $Fe^{2+/3+}$, TiO_2) have been added in order to attain better treatment performances, these technologies being known as advanced oxidation processes (AOPs). UV light emitting diodes (LEDs) have received a great deal of attention in the last years in this domain, namely for water and wastewater treatment, especially due to its ecofriendliness (by replacing mercury) and long-life time. In comparison to traditional UV lamps, the electricity is more efficiently converted into light, with the possibility of adjusting the irradiance. Emerging applications include pulsed light in water treatment due to the nearly instantaneous switching of these irradiation sources [20,21]. UVA-LEDs with emission around 360–390 nm have been selected in different photocatalytic studies [20–26]. Efforts to optimize the TiO_2-photocatalytic treatment with UV-LEDs, have been done in the last years [27]. Photocatalytic disinfection using TiO_2 and traditional UV lamps has been widely reported [28–30], but only a few publications have implemented UVA-LEDs and they are limited to *E. coli* [21,31].

The aim of the present study is to simultaneously remove antibiotics and ARB from secondary UWW. Azithromycin (AZT), trimethoprim (TMP), ofloxacin (OFL) and sulfamethoxazole (SMX) were selected as model antibiotics because they represent distinct classes and are among the most used antibiotics to treat human and veterinary infections [1,4]. The novel aspects of this study include the first evaluation of the antibiotics and ARB removals from real UWWs using UVA-LEDs in the TiO_2-photocatalytic treatment. The scavenging effect of methanol (MeOH) as a carrier solvent in photocatalytic kinetic parameters was also addressed.

2. Materials and methods

2.1. Chemicals and materials

AZT (CAS number 117772-70-0), TMP (CAS number 738-70-5), OFL (CAS number 82419-36-1), SMX (CAS number 723-46-6), clindamycin (CLI, CAS number 18323-44-9), and deuterated internal standards (azithromycin-d3 and ofloxacin-d3), all with > 98% purity, were purchased from Sigma-Aldrich. A methanolic stock solution containing AZT, TMP, OFL and SMX (150 mg L^{-1} each) was prepared to be used in the spiked experiments.

TiO_2 (80% anatase, 20% rutile) was supplied by Evonik Degussa GmbH (P25). MeOH and acetonitrile (MS grade) were obtained from VWR International (Fontenay-sous-Bois, France). Ethanol (HPLC grade) was acquired from Fisher Scientific (Leicestershire, UK), whereas formic and sulfuric acid were obtained from Merck (Darmstadt, Germany). Oasis® HLB (Hydrophilic-Lipophilic Balanced) cartridges (150 mg, 6 mL) used for sample preparation, were purchased from Waters (Milford, MA, USA). MilliQ water system provided ultrapure water with resistivity > 18 MΩ cm at 25 °C.

The culture media Tryptone Bile X-Glucuronide Agar (TBX) and Plate Count Agar (PCA) were provided by Sigma-Aldrich, and m-Enterococcus Agar (m-Ent) was supplied by Difco (Maryland, USA).

2.2. Wastewater sampling and characterization

Secondary UWW was collected at the effluent of the secondary settling tank of an UWWTP located in Northern Portugal (average monthly flow of 25,707 ± 3,570 m^3 day^{-1}), in three sampling occasions: September-December 2017 (spiked tests), January-March 2018 (non-spiked tests), April-May 2018 (disinfection tests). Wastewater characteristics can be found in Table S1.

2.3. Experimental setup, radiation measurements and absorption–scattering model

The lab-scale batch experiments were run in a 150 mL reactor (5 cm out diameter, 3.8 cm inner diameter and 16.0 cm height at maximum filling, Fig. S1a). Four UV high intensity LEDs (working at 9 W) and the respective heatsink/fan cooling systems (1 W) were placed on four lateral sides of a cubic box containing the annular photocatalytic reactor (Fig. S1a). Each LED (15.5 mm × 23 mm) had a dominant emission line at 381 nm (Fig. S1b) and long service life, with an intensity above 70% after 10,000 h work. The distance between each LED and the reactor was set at 3.3 cm (at a height of 10 cm). Three main radiation configurations were tested, namely switching on a single LED, two LEDs placed perpendicularly to each other, or the four LEDs (Fig. S2a–c). All the radiation measurements were performed using a spectrometer (Ocean Optics USB2000 +) equipped with cosine corrector and the software *Spectra Suit*. The spectral intensity of radiation (W m^{-2} nm^{-1}) and the spectral emitted radiant energy (μJ nm^{-1}) of each LED were measured with the probe at 3.3 cm distance from the LED (i.e., at the reactor wall). The procedure for the calculation of emitted radiant energy is reported in Supplementary Information (Text S1. Emitted radiant energy). Moreover, the irradiance (W m^{-2}) was recorded by varying the position of the probe in a parallel plane at the same 3.3 cm distance. The UV dose provided by each single LED (in the red zone of Fig. S1c) is given by the time of light exposure multiplied by the average value of irradiance (considering the irradiated surface). The procedure for the calculation of average value of irradiance is reported in Supplementary Information (Text S2. Average irradiance). Optical thickness (τ) at 10 cm of height (central point of red zone, Fig. S1c) is calculated through Eq. (1):

$$\tau = \delta\, C_{cat}\, \beta \quad (1)$$

where δ is the thickness of wastewater being irradiated, C_{cat} is the catalyst load and β is the spectral average value of extinction coefficient of the photocatalyst given by Eq. (S3) (Text S3. Average extinction coefficient) [30]. Considering a neglected irradiance gradient across the wastewater (low thickness annulus), β is only function of radiation field and specific extinction coefficient values (β_λ) of photocatalyst in water [32].

The reactor configuration is modelled as a thin-film annular photoreactor (thickness of annulus, δ = 0.005 m, considering radius and

thickness of internal and external walls) but using external light source [33]. UVA light absorption of the external wall (PYREX®) is negligible and spectral intensity after the external wall is expected to be similar.

2.4. Degradation of antibiotics

UWW samples were spiked with the antibiotics following a procedure described elsewhere [25]. Briefly, 0.1 mL of the methanolic stock solution (150 mg L^{-1} of each antibiotic) was added to an empty volumetric flask, the residual solvent was evaporated using a nitrogen flow, and 150 mL of UWW were added into the flask, which was stirred and sonicated for 30 s, giving an initial concentration of 100 μg L^{-1} of each antibiotic in the spiked UWW. Dissolved organic carbon (DOC) analyses were performed to confirm MeOH evaporation, based on the comparison of the values obtained in spiked and non-spiked UWW samples. Similar values were expected, since the contribution of the spiked antibiotics to the DOC content was considered to be negligible (1.9%).

Different TiO_2 catalyst loads (0.10, 0.25, 0.50, 1.00, 1.50, and 2.00 g L^{-1}) and number of LEDs (1, 2 and 4 LEDs) were investigated for the removal of antibiotics in spiked UWW, under continuous magnetic stirring and air-sparging (3.5 L min^{-1}). After a 30 min dark adsorption period in the reactor, an aliquot of 15 mL was withdrawn for DOC analysis and the lamp jacked was inserted. Photocatalytic degradation was studied at regular treatment times (0, 15, 30, 60, 120 and 180 min), by withdrawing 1 mL aliquots from the reactor. These aliquots were centrifuged at 13,500 rpm during 10 min, being the supernatant analysed by Ultra-High-Performance Liquid Chromatography with tandem Mass Spectrometry (UHPLC-MS/MS). Photolysis was evaluated during 180 min, using the conditions described above in the absence of TiO_2. For the scavenging study, 75 μL of MeOH was added to the spiked UWW sample (reaching a MeOH concentration of 0.4 g L^{-1}, 0.05% v/v, equivalent to ca. 150 mg L^{-1} of DOC).

Photocatalytic experiments using real non-spiked UWW were carried out with 4 LEDs and 1.00 g L^{-1} of catalyst. Dark adsorption on TiO_2 suspended in UWW was evaluated in 1 L glass bottles covered by aluminum foil. After 24 h of adsorption–desorption equilibrium, a volume of 135 mL of UWW was transferred to the annular reactor, where photocatalytic experiments took place. Different treatment times (0, 5, 10, 15, 30, 60, and 120 min) were tested in distinct assays, since the volume required of filtered treated samples (1.2 μm glass microfiber filters GF/C, 47 mm; Whatman™, UK) for solid phase extraction (SPE) was 100 mL. All assays were performed in triplicate.

2.5. Disinfection studies

Disinfection of real UWW was investigated after 60 min of photocatalytic treatment, using wastewater samples collected in different days. Freshly collected secondary UWW was stirred for 30 min in 1 L bottles in the dark (with and without TiO_2) and aliquots of 135 mL were loaded into the annular reactor. The same operating conditions described in Section 2.4 for the non-spiked experiments were used in disinfection studies (4 LEDs and 1.00 g L^{-1} of catalyst). Control experiments in the absence of catalyst (photolysis) and in the absence of light but with catalyst (dark adsorption) were carried out for the same 60 min. Volumes of 1 or 10 mL were collected after 60 min of photocatalytic treatment. The potential regrowth of bacteria in photocatalytic treated UWW and in the respective controls, after 3-day storage in the dark at room temperature (24 °C), was evaluated. Total and antibiotic resistant bacteria were enumerated based on the membrane filtration method.

2.6. Analytical methods

The antibiotics were quantified by UHPLC-MS/MS, using a Shimadzu apparatus equipped with a Kinetex™ XB-C18 100 Å column (100 × 2.1 mm i.d.; 1.7 μm particle diameter) supplied by Phenomenex, Inc. (Torrance, CA, USA). Ultrapure water and a mixture of MeOH and acetonitrile (50/50, v/v), both containing formic acid (0.1%, v/v), were used as mobile phase in isocratic mode (20/80 v/v) at a flow rate of 0.3 mL min^{-1}. Column oven and autosampler temperatures were set at 35 and 4 °C, respectively. The injection volume was 20 μL. For non-spiked experiments, the samples were previously concentrated and cleaned-up by SPE before UHPLC-MS/MS analysis, by using OASIS® HLB cartridges to extract the target antibiotics from 100 mL of real UWW [34]. Briefly, the samples were acidified to pH 3 using sulfuric acid and supplemented with 20 μL of a solution containing 5 mg L^{-1} of each deuterated internal standard, consisting of azithromycin-d3 and ofloxacin-d3. The acidified samples were passed through the cartridges at a constant flow of 10 mL min^{-1}, previously conditioned with ethanol and ultrapure water (4 mL each). After the washing step with 4 mL of ultrapure water and subsequent drying, 4 mL ethanol were used as elution solvent and the eluate was collected in glass tubes. The extracted solution was dried in a Centrivap Concentrator® device (LABCONCO® Corporation, Kansas City, MO, USA), during 120 min at 45 °C. The dried extracts were dissolved in 250 μL of ethanol and the resulting solution was filtered through 0.22 μm polytetrafluoroethylene syringe filters (Membrane Solutions, Kent, WA, USA), and further analysed by UHPLC-MS/MS (conditions in Tables S2 and S3).

The DOC of samples was measured before the experiments by using a Shimadzu TOC-L analyzer.

2.7. Bacterial count

The culture medium PCA (for total heterotrophs), and the selective media m-Ent (for enterococci) and TBX (for *E. coli*), supplemented or not with antibiotics, were used for the enumeration of resistant and total bacteria, respectively, by the membrane filtration method as described by Novo et al. [35]. Antibiotics were sterilized by filtration (0.22 μm porosity) prior to addition to the sterilized culture media. AZT (stock solution prepared in ethanol) was added to TBX to reach a concentration of 32 mg L^{-1}; OFL (stock solution prepared in distilled water adding dropwise 4 g L^{-1} NaOH until total dissolution) was added to m-Ent for a final concentration of 4 mg L^{-1}; and SMX (stock solution prepared in distilled water adding dropwise 100 g L^{-1} NaOH until total dissolution) was added to PCA to reach a concentration of 512 mg L^{-1}. The selected concentrations were in accordance with epidemiological cut-off values [36].

Samples or serial 10-fold dilutions were filtrated through cellulose nitrate membrane filters (0.22 μm porosity, Biotech, Germany), which were placed on the respective culture medium and incubated at temperature and time, as follows: 30 °C and 24 h for PCA and PCA + SMX; 37 °C and 24 h for TBX and TBX + AZT; and 37 °C and 48 h for m-Ent and m-Ent + OFL. All assays were performed in triplicate. The ratio between the number of colony forming units (CFU) on antibiotic supplemented and non-supplemented media was used as an indicator of the resistance percentage.

2.8. Statistical analysis

CFU (log value) of total bacteria, resistant bacteria and their ratio, corresponding to each experiment or control were compared by single factor analysis of variance (ANOVA), followed by post-hoc Tukey's test using the software SPSS (Version 25.0 for Windows). The significance level was set to 0.05.

3. Results and discussion

3.1. Photodegradation of antibiotics

The degradation efficiencies by UVA of the antibiotics spiked in UWW, in the absence of MeOH and using 4 LEDs, revealed the following resilience order: TMP ≈ SMX > AZT > OFL (Fig. 1). Owing to the low absorbance above 290 nm wavelength [37–39], many antibiotics are recalcitrant to photolysis (e.g., macrolides, sulfonamides and

pyrimidine). However, real matrices can play an important role on their indirect photodegradation, exceptions being found in some cases as fluoroquinolones, which are reported to be more susceptible to UV photolysis in pure water than in UWW [38,40]. Thus, indirect photolysis can take place by means of some inorganic species and/or the effluent organic matter (EfOM) present in UWW, as well as by its excited triplet sate ($^3EfOM^*$) [41]. For instance, degradation of the zwitterionic form of OFL at pH 7.7 was reported under solar light [40], the natural dissolved organic matter and OFL being suggested to compete for absorption of photons, as fluoroquinolones in general [39]. In contrast, $HO^{\cdot}/CO_3^{\cdot -}$ radicals were proposed as the main species involved in the mechanism of TMP photodegradation in secondary UWW under solar light, whereas $^3EfOM^*$ was responsible for the AZT elimination [42]. Another study has also reported that natural organic matter (humic acids) favours the degradation of AZT under solar photolysis in certain conditions [43].

Regarding the effect of MeOH on photolysis (Table 1, Fig. S3), this solvent (0.05% v/v) did not markedly disturb the above mentioned order of resilience for these antibiotics (TMP > SMX > AZT ≈ OFL), but affected the values of the respective apparent first-order reaction rate constants (k): k_{OFL} increased slightly, k_{AZT} and k_{SMX} increased 2.5 and 9 times, respectively, whereas k_{TMP} decreased 7 times. Because the degradation rate of AZT and SMX is much higher in UWW with MeOH (Fig. S3) than in UWW (Fig. 1a), it seems that MeOH promotes $^3EfOM^*$ in UVA photolysis. On the other hand, TMP was the most resilient to UVA photolysis, but in the presence of MeOH its degradation is even slower. MeOH did not remarkably modify the rate in the case of OFL. Accordingly, scavenging studies have already revealed that singlet oxygen is the main reactive oxygen species responsible for the degradation of OFL [44], and of most fluoroquinolones, such as levofloxacin, gatifloxacin, difloxacin and balofloxacin [39], suggesting also that the $^3EfOM^*$ degradation pathway is not dominant. In fact, photo-oxidation resulting from reactive oxygen species photochemically generated from the oxygen dissolved in the reaction mixture was already shown in a previous study [44].

3.2. Radiation absorption-scattering model

The UVA-LEDs (lower cost and higher power efficiency than UVC- and UVB-LEDs [26]) present the main emission peak at 381 nm (Fig. S1b), overlapping with the tail of the TiO_2 absorption spectrum (380 nm, [45]). The total emitted radiant energy (11.7 μJ) and its fraction (4.2 μJ) with photons having an energy higher than the bang gap of the photocatalyst (3.2 eV, [45]) is shown in Fig. S1b, while the procedure for its estimation is described in Supplementary Information (Text S1. Emitted radiant energy).

According to the nature of the LED light (beam) and its viewing half angle (ca. ± 30°), only a part of the external reactor surface (4 cm diameter circle orthogonally projected on the cylindrical surface) is irradiated by the UVA light. The main ranges of irradiance (Fig. S1c) are: 515–250 W m^{-2} (2 cm diameter red circle), 250–15 W m^{-2} (3 cm diameter orange circular crown) and 15–1 W m^{-2} (4 cm diameter yellow circular crown). The UV dose provided by a single LED in the red zone (area similar to a circle in a plane, ca. 3.14 cm^2) for an hour of light exposure is ca. 1,220 kJ m^{-2}. Since light uniformity also plays a key role in the efficiency of the process, systems based on LEDs must be properly designed in order to illuminate the entire reactor volume [31].

Several studies have shown how important is the catalyst load, with low amounts permitting radiation losses due to the transparency of the solution, while an excess promoting screening effects due to the opacity of the solution, hampering the optimal irradiation of catalyst at the

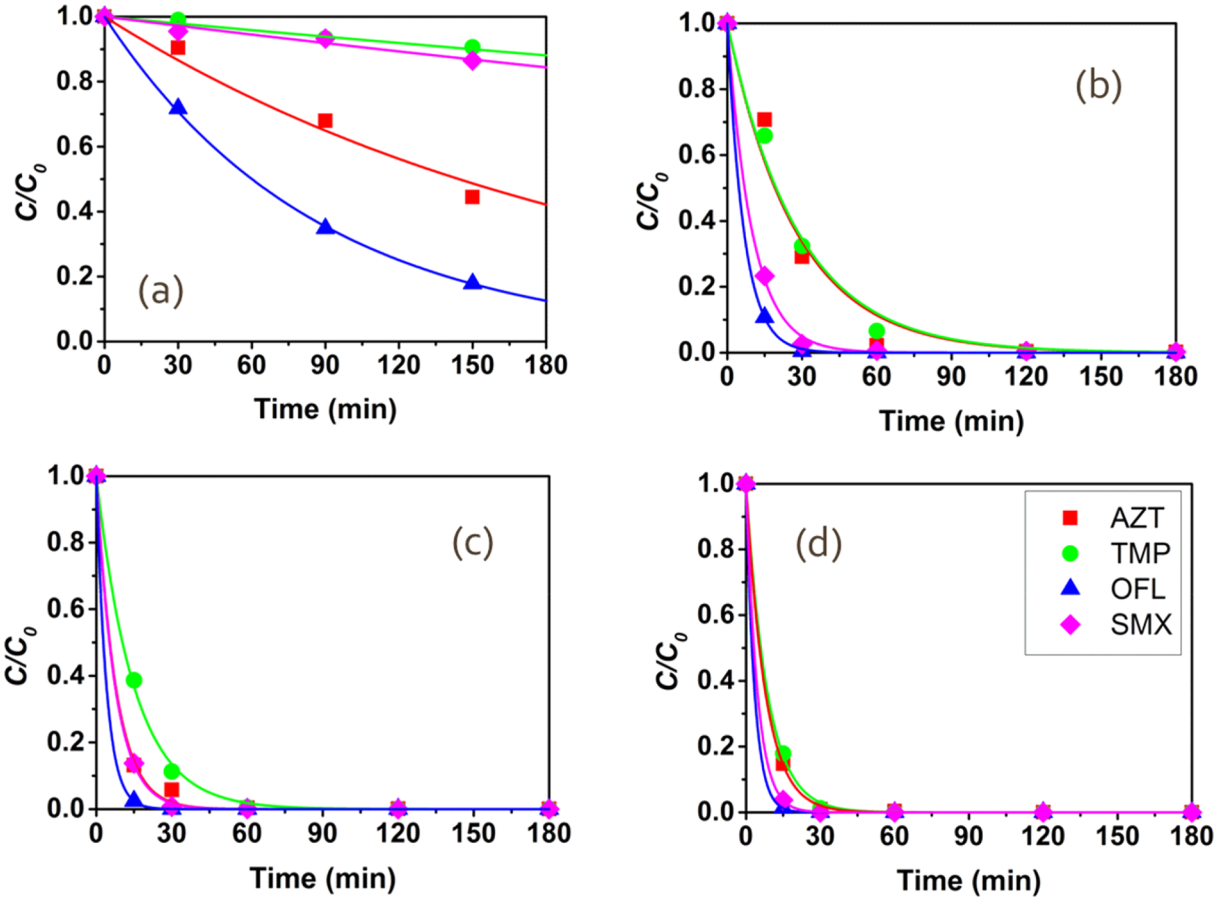

Fig. 1. Removal efficiencies of AZT, TMP, OFL and SMX spiked in UWW (100 μg L^{-1} without MeOH) by using 4 LEDs without catalyst (a) and 1 (b), 2 (c) and 4 LEDs (d) in photocatalytic experiments (catalyst load set at 1.00 g L^{-1}).

Table 1
Apparent first-order reaction rate constant (k), as function of optical thickness and catalyst load, considering different number of LEDs in different matrices.

Matrix	Optical thickness (−)	Catalyst load ($g\,L^{-1}$)	$k \times 10^3$ (min^{-1})											
			1 LED				2 LEDs				4 LEDs			
			AZT	TMP	OFL	SMX	AZT	TMP	OFL	SMX	AZT	TMP	OFL	SMX
Spiked WW (w/o MeOH)	0.00	0.00									4.8	0.7	11.5	0.9
	0.97	0.10									29.2	14.3	47.5	25.5
	2.43	0.25									56.8	38.0	108.7	75.7
	4.86	0.50									67.6	56.9	180.2	105.0
	9.73	1.00	36.3	35.4	149.7	100.3	129.8	66.8	248.5	133.6	129.1	117.1	290.5	212.6
Spiked WW (MeOH)	0.00	0.00	4.8	0.3	3.8	1.3	3.5	0.5	5.7	3.6	12.0	0.1	13.0	8.1
	0.97	0.10	a	a	a	a	13.6	2.2	21.6	9.7	13.3	5.2	41.6	14.1
	2.43	0.25	6.6	3.4	29.4	17.0	10.9	5.7	39.7	19.1	26.4	8.9	69.8	34.4
	4.86	0.50	12.7	4.7	45.1	27.0	18.8	7.6	82.2	48.1	18.3	14.3	111.8	53.5
	9.73	1.00	15.4	7.9	76.5	53.7	32.5	13.4	171.1	83.1	67.0	23.5	269.6	144.4
	14.59	1.50	27.4	11.7	126.6	100.2	45.8	20.6	211.8	178.8	66.0	29.0	264.3	b
	19.46	2.00	19.6	11.5	135.2	104.0	57.6	17.9	273.7	228.8	43.6	33.4	301.9	b
Actual WW	9.73	1.00									64.6[d]	128.2[d]	363.7[d]	c

a, not determined; b, lack of data (removal in less than 5 min); c, initial concentration below the limit of quantification; d, C_0 is different for each antibiotic.

inner side of the reactor [30,33,46]. Thus, to maximize the antibiotics' removal, it is recommended that all catalyst active sites are available, the photocatalytic efficiency being governed by the catalyst load, light irradiation and reactor geometry [46]. Optical thickness (τ, Eq. (1)) considers all these three parameters. Since radiation field is not constant along the reactor, τ is estimated only for the central red parts of Fig. S1c (irradiance of $515\,W\,m^{-2}$). The radiation field (spectral intensity, Fig. S1b) together with the β_λ values [32] gives a β of ca. 1, $950\,m^2\,kg^{-1}$ according to the model proposed by Rizzo et al. [30]. Once calculated δ (0.005 m) and β, the values of τ for each catalyst load are reported in Table 1. According to Li Puma and Brucato [33], for the scattering albedo of TiO_2 (ca. 0.74), radiation transmission factor is maximized at $\tau > 6$, meaning for the present configuration a catalyst load between 1.00 and $2.00\,g\,L^{-1}$.

3.3. Photocatalytic degradation of antibiotics in spiked UWW

The results obtained for the photocatalytic treatment of spiked UWW are shown in Figs. 1–3 and Figs. S3–S5. In the absence of MeOH (Figs. 1b–d and 2), the general resilience order (TMP ≈ AZT >

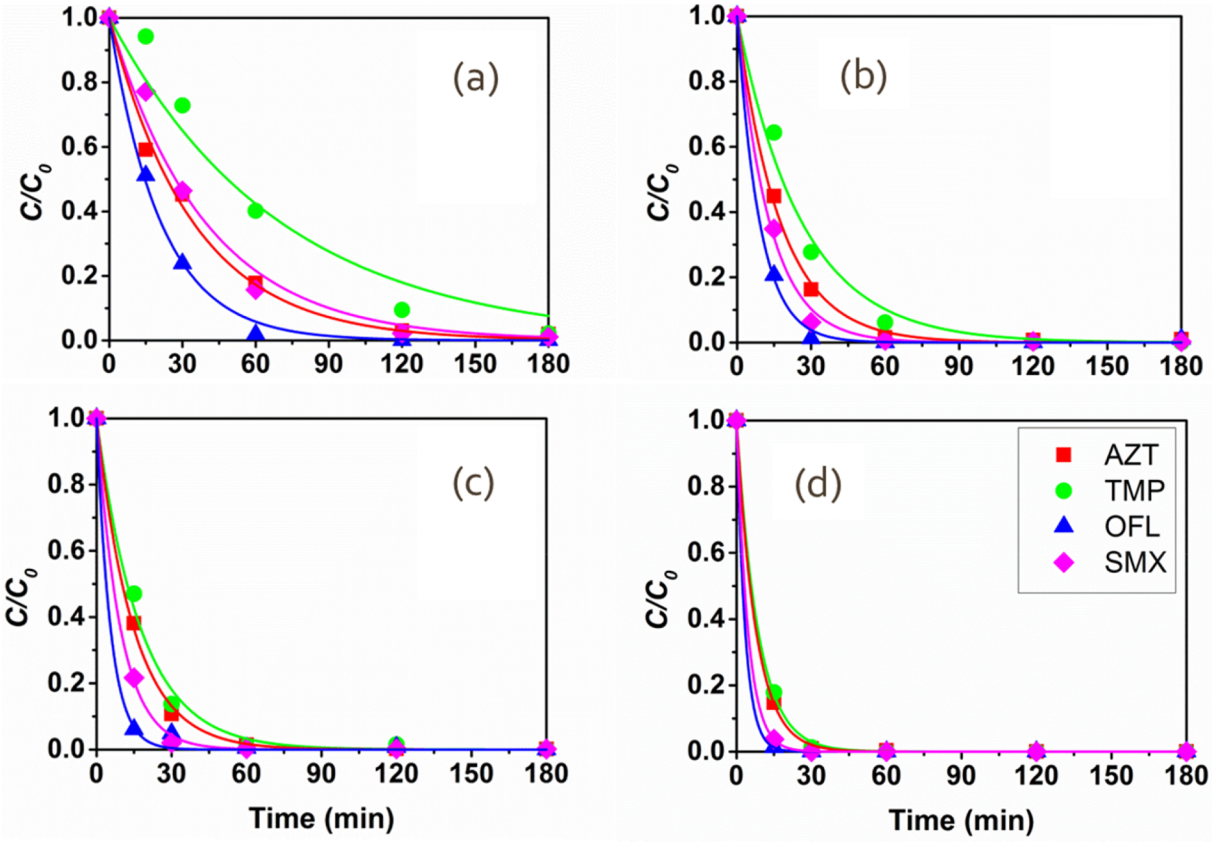

Fig. 2. Removal efficiencies of AZT, TMP, OFL and SMX spiked in UWW ($100\,\mu g\,L^{-1}$ without MeOH) by photocatalysis using 0.10 (a), 0.25 (b), 0.50 (c) and $1.00\,g\,L^{-1}$ (d) catalyst load (number of LEDs set at 4).

SMX > OFL) was slightly different from that obtained by photolysis (Fig. 1a). Moreover, it was generally observed that the degradation rates of all antibiotics increased linearly with the number of LEDs and catalyst load up to 1.00 g L^{-1}, either in the absence or presence of MeOH (Fig. 3a, b). The 4-LEDs configuration allowed the largest irradiated solution volume, since each LED irradiated a specific section of the reactor (Fig. S2c). Moreover, the k values obtained when using 2 LEDs with 2.00 g L^{-1} of catalyst (Fig. S4b) and 4 LEDs with 1.00 g L^{-1} of catalyst (Fig. S4c) were similar for most antibiotics. These observations support the existence of a heterogeneous photocatalytic regime.

In all the photocatalytic tests performed using MeOH as radical scavenger, the k values determined for all the antibiotics were lower than those in the absence of MeOH, but the same order was observed for the degradation rates (Fig. 3). TMP keeps being the most resilient compound and its k values were those mostly affected by the presence of the organic solvent, indicating a higher susceptibility to $HO^{\cdot}$ radicals than the other antibiotics under study. For instance, using 4 LEDs and 1.00 g L^{-1} of catalyst, k_{TMP} increased from 0.0235 min^{-1} (in the presence of MeOH) to 0.1171 min^{-1} (in the absence of MeOH) (Fig. 3a). A recent study on the influence of carrier solvent [25] highlighted the influence of MeOH on the photocatalytic degradation of water micropollutants (including SMX and TMP).

Regarding the photocatalytic degradation of OFL (1.00 g L^{-1} of catalyst), the difference between k_{OFL} in the presence and absence of MeOH is not markedly different in the case of 4 LEDs, compared to the results obtained with 1 and 2 LEDs (Fig. 3a). Interestingly, Hapeshi et al. [44] suggested that valence band holes are the primary photocatalytic oxidation pathway of OFL in ultrapure water, since OFL reaction rate in neutral and acidic pH was higher than at a basic pH > 8 where OFL molecules (cationic form) are expected to be attracted to TiO_2 (anionic form), and $HO^{\cdot}$ radicals are more likely produced.

3.4. Photocatalytic degradation of antibiotics in non-spiked UWW

Three different sampling campaigns of secondary UWW were performed during the winter of 2017/2018 in a UWWTP located in Northern Portugal. The initial concentration of SMX was below the limit of quantification (LOQ) in all samples. Considering that CLI was always present in the UWW collected in this UWWTP, its concentration was quantified in the next experiments, together with AZT, TMP and OFL. The measured concentrations followed the general decreasing order: AZT > OFL > TMP > CLI, these concentrations being more variable for AZT (369–1686 ng L^{-1}) and OFL (105–648 ng L^{-1}).

The samples from the first campaign (UWW1, Fig. 4) were used to compare the effect of 10 min photolysis with 10 min photocatalysis after adsorption in the dark for 24 h. Photolysis and adsorption had a similar performance in removing AZT, TMP and OFL, since photolysis led to abatements ranging from 33 ± 16% to 47 ± 3%, whereas the removal by adsorption varied between 41 ± 12% and 62 ± 9%. Both photolysis and adsorption steps had negligible effect over the CLI concentration. In contrast, the photocatalytic degradation of TMP, OFL and CLI was very fast, the concentrations reaching values below the LOQs in less than 10 min. In fact, only AZT could be quantified after the photocatalytic treatment, but at very low concentrations.

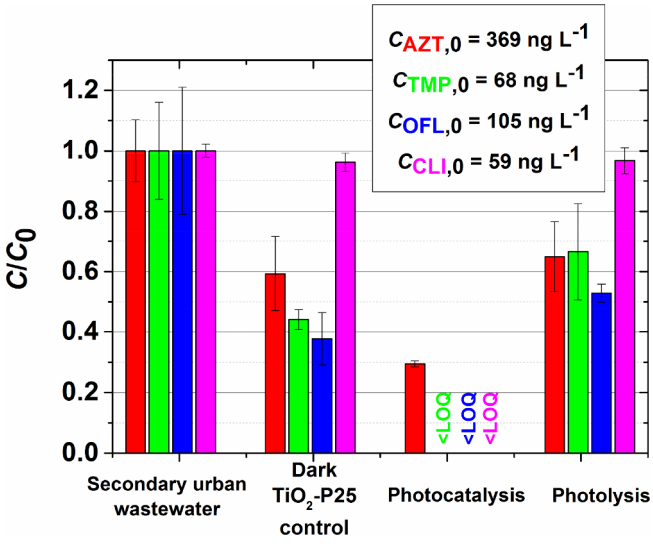

Fig. 4. Normalized concentrations of AZT, TMP, OFL and CLI in UWW1 after 1 day of adsorption in the dark with TiO_2, and 10 min of photocatalytic and photolytic treatment.

The concentrations were nearly two times higher in the second sampling campaign (UWW2, Fig. 5a), except for CLI which was quantified at levels similar to that found in UWW1. As in the first campaign, a remarkable adsorption (28 ± 2% for AZT, 62 ± 13% for TMP and 51 ± 7% for OFL) was found for all the antibiotics except for CLI (15 ± 1% only in UWW2). After treatment of UWW2 by photocatalysis, OFL and CLI were removed to levels below the LOQs, AZT and TMP being quantified at low concentrations after the photocatalytic treatment.

Higher concentrations of AZT and OFL were found in the third sampling campaign (UWW3, Fig. 5b), an intermediate level of TMP and the same concentration of CLI. The average removals by adsorption in UWW3 were similar to those obtained in the other samples (36 ± 1% for AZT, 38 ± 1% for OFL and negligible in the case of CLI), with exception of TMP (21 ± 9%) which might be attributed to the sample

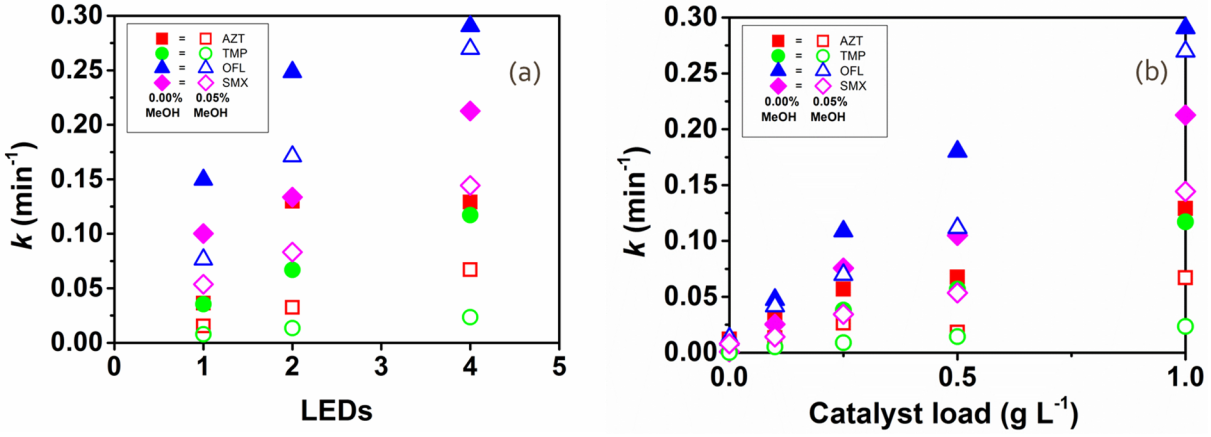

Fig. 3. Apparent first-order reaction rate constant (k) of AZT, TMP, OFL and SMX spiked in UWW (100 µg L^{-1}, with (open symbols) and without methanol (solid symbols)) by photocatalysis: varying the number of LEDs and using a catalyst load set at 1.00 g L^{-1} (a); and using 4 LEDs and varying the catalyst loads (b).

heterogeneity. Once again, the photocatalytic treatment allowed to decrease the concentrations of OFL and CLI to levels below the LOQs, whereas AZT and TMP were quantified at low concentrations. The variations on the concentrations of these antibiotics during the photocatalytic treatment of UWW3 is represented in Fig. 5c for AZT and OFL and Fig. 5d for TMP and CLI. The required treatment time to reach the antibiotic concentration under the LOQ in UWW3 was 60 min and 15 min for AZT and TMP respectively, and 10 min for both OFL and CLI.

The degradation kinetics of AZT, TMP and OFL at actual concentrations in UWW (ng L^{-1} levels) were compared to those obtained in spiked UWW (100 µg L^{-1}) when the treatment was performed in the absence of MeOH. According to Malato et al. [45], the rate constants of micropollutants usually increase with the initial substrate until reaching a steady-state (saturation level of Langmuir-Hinshelwood kinetic model). However, in the present study, this was observed only for k_{AZT} (ca. 100% increase). No relevant difference of k_{TMP} (ca. 10% decrease) and a significant decrease of k_{OFL} (ca. 20%) were found between non-spiked and spiked (absence of MeOH) tests (Table 1). In fact, AZT was also more resilient than TMP in another study using a UVA artificial lamp and 0.5 g L^{-1} of TiO_2 for the removal of emerging contaminants at real concentrations in UWW [47]. Moreover, the removal reported for OFL (84%) was also higher than that achieved for TMP (70%) in other study, after 8 h treatment using a compound parabolic collector and a very low amount of TiO_2 (0.02 g L^{-1}) in solar photocatalysis [48]. AZT and TMP have been widely reported as recalcitrant compounds when using AOPs [13], while quinolones are more susceptible to degradation than AZT and TMP, for instance by UVC irradiation of UWW [49].

3.5. Disinfection, antibiotic resistance prevalence and bacterial regrowth

AOPs are promising processes for bacterial inactivation in UWW, although ARGs are detected after treatment, a fact that is worsened by bacterial regrowth and bacterial community disturbance [16,50–52], thus increasing the risk of antibiotic resistance spread. Among the different AOPs, photo-Fenton, UV/H_2O_2 and heterogeneous photocatalysis (UV/TiO_2) have been tested for the inactivation of different bacterial groups [7,53]. However, the literature reports mainly the assessment of the efficiency of LEDs-driven TiO_2-photocatalysis on disinfection of UWW based on the monitoring of *E. coli* suspensions [21,31]. Recently, it was demonstrated that when using TiO_2 as photocatalyst in aqueous solution, a LED system was more efficient than traditional lamps if the same UV dose is applied for a shorter period but with higher intensity, leading to high *E. coli* inactivation rates [31], an additional advantage being the possibility of applying a periodic intense radiation [21].

In this study, the performance of 4 LEDs photolysis and 4 LEDs photocatalysis (using a catalyst load of 1.00 g L^{-1}) to reduce the counts of viable total heterotrophs, *E. coli* and enterococci and their antibiotic resistant counterparts in UWW samples, was assessed. CFUs were enumerated before and immediately after treatment, and after 3-day storage in the dark, at room temperature (Fig. 6). Initial load of total heterotrophs, *E. coli* and enterococci in secondary UWW were 7.7 ± 0.2, 5.9 ± 0.4 and 5.7 ± 0.3 log (CFU / 100 mL), respectively. The percentage of SMX resistant heterotrophic bacteria and AZT resistant *E. coli* in the secondary UWW was 8.7 ± 2.9% and 1.9 ± 1.5%, respectively (Table S5). These values of sulfonamide resistant heterotrophs [35,54] and AZT resistant *E. coli* [55] are in agreement with previous studies. The percentage of OFL resistant enterococci was lower (1.5 ± 0.2%) (Table S5) than that reported by Michael et al. [56] (ca. 20%), probably because a 4 times higher OFL concentration (based on the epidemiological cut-off values [36]) was used in the culture media in the present study.

A reduction on the load of the analysed bacterial groups was observed for both photolytic and photocatalytic processes, with higher

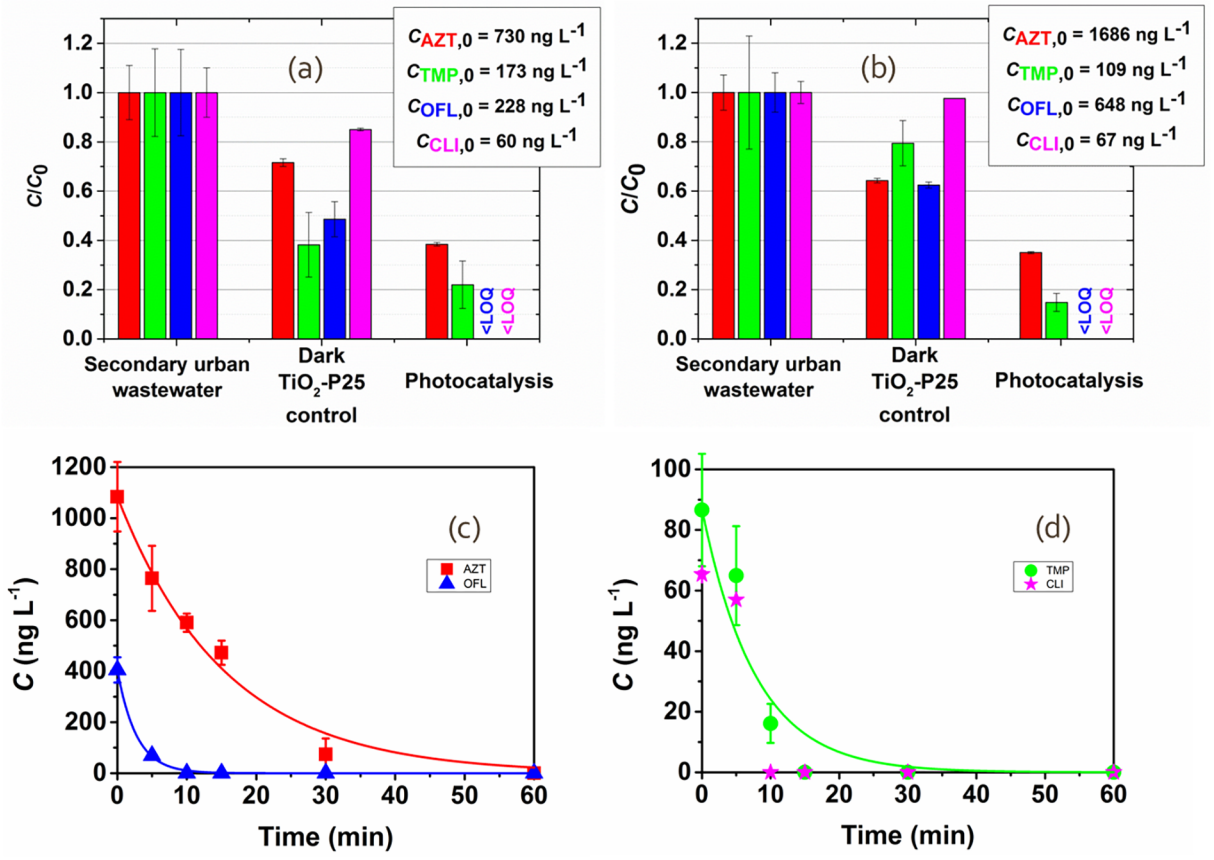

Fig. 5. Normalized concentrations of AZT, OFL, TMP and CLI after adsorption in the dark (TiO_2, 1 day) and 10 min of photocatalytic treatment of UWW2 (a) and UWW3 (b). Evolution of concentrations of AZT and OFL (c), TMP and CLI (d) in UWW3 during photocatalytic treatment.

inactivation rates for photocatalysis (Fig. 6, Table S4). The efficiency of photolysis on the bacterial load reduction of the studied bacteria followed the order: heterotrophs (1.6 ± 0.6 log reduction) > *E. coli* (1.4 ± 0.7 log reduction) > enterococci (1.0 ± 0.3 log reduction). Regarding antibiotic resistant groups, photolysis performance followed the order: *E. coli* (2.5 ± 0.2 log reduction) > enterococci (1.5 ± 0.6 log reduction) ≈ heterotrophs (1.4 ± 0.4 log reduction). Concerning the photocatalytic treatment, the following order was found: heterotrophs (2.7 ± 0.6 log reduction) > *E. coli* (2.3 ± 0.3 log reduction) > enterococci (2.0 ± 0.2 log reduction) and resistant groups (*E. coli* (2.5 ± 0.4 log reduction) ≈ enterococci (2.4 ± 0.7 log reduction) > heterotrophs (2.3 ± 0.5 log reduction)). The bacterial loads of the control samples, with and without the addition of photocatalyst, were not observed to vary significantly.

Because of the bacterial load variations, the percentage of ARB decreased after photolysis for *E. coli* (from 1.9 ± 1.5% to 0.4 ± 0.4%) and increased after photocatalysis for heterotrophs (from 8.7 ± 2.9% to 23.6 ± 18.3%) (Fig. 6, Table S5). Other studies assessing the SMX resistant fraction of total heterotrophs after UVC irradiation [54] and OFL resistant fraction of enterococci [56] after solar photo-Fenton did not report variations with respect to the initial resistance percentage. Nevertheless, some authors observed faster inactivation of macrolide resistant *E. coli* than of susceptible *E. coli* counterparts in UWW treated by solar TiO_2 photocatalysis [57].

Despite the observed inactivation of the analysed microbial groups, it was hypothesized that at least some bacteria might have become transitorily unculturable, although maintaining the capacity to regrow, as reported before [22,58–60]. Regrowth is mainly attributed to survival and capacity to use available carbon sources generated during the oxidation of recalcitrant organic matter [58,61]. When compared to the UWW immediately after the photolysis treatment, the loads of total heterotrophs increased (1.1 ± 0.9 log higher), and the loads of total enterococci decreased (0.8 ± 0.5 log lower) after storage, whereas no significant changes in the abundance of total *E. coli* were found. Regarding antibiotic resistant counterparts, only enterococci showed a significant change (0.9 ± 0.6 log reduction) after storage. In the photocatalytic treated stored water, the loads of both the total heterotrophs and total *E. coli* were higher than immediately after the treatment (3.4 ± 0.7 and 0.7 ± 0.9 log higher, respectively), whereas no significant changes were observed for total enterococci. Regrowth of resistant heterotrophic bacteria was observed in the stored water treated by photocatalysis (2.5 ± 0.6 log increase), while no significant changes were found for resistant *E. coli* and resistant enterococci. Photocatalysis treated water seems to support higher regrowth than photolysis, suggesting that this treatment may increase the biodegradable organic matter more than photolysis [61]. In the non-treated controls, the abundance of all analysed microbial groups was maintained or decreased with storage.

Due to the variations pointed out above, when compared to secondary treated UWW, the stored UWW after photolysis showed lower loads of total *E. coli* (1.8 ± 0.4 log reduction) and total enterococci (1.8 ± 0.2 log reduction), with no significant reduction for total heterotrophs. Also the loads of the resistant bacterial groups were lower in the stored water than in the secondary treated UWW: enterococci (2.5 ± 0.2 log reduction) > *E. coli* (1.7 ± 0.3 log reduction) > heterotrophs (0.9 ± 0.9 log reduction). Similarly, in the stored UWW after photocatalysis only total enterococci and total *E. coli* were less abundant than in the original secondary UWW (1.7 ± 0.4 and 1.4 ± 0.7 log reduction respectively), while total heterotrophs did not show significant changes. A similar trend was found for the antibiotic resistant groups, with lower loads of enterococci (3.0 ± 0.3 log reduction) and *E. coli* (2.0 ± 0.7 log reduction), and no significant changes in the load of heterotrophs.

Due to these variations, the percentage of OFL resistant enterococci in the stored treated wastewaters was significantly lower (photolysis: 0.4 ± 0.4%; photocatalysis: 0.1 ± 0.1%) than in the original secondary UWW (1.5 ± 0.2%) (Fig. 6, Table S5). Fecal organisms, mainly enterococci, seem to be more vulnerable to disinfection (photolysis and photocatalysis) than total heterotrophs, probably due to the fact that they are at a lower abundance or because bacteria of this bacterial group are susceptible to permanent damage, as described in the literature [16,28,62].

4. Conclusion

The variability of antibiotic concentrations for different real UWW matrices coming from the same UWWTP constitutes no obstacle to their efficient degradation by TiO_2-heterogeneous photocatalysis using UVA-

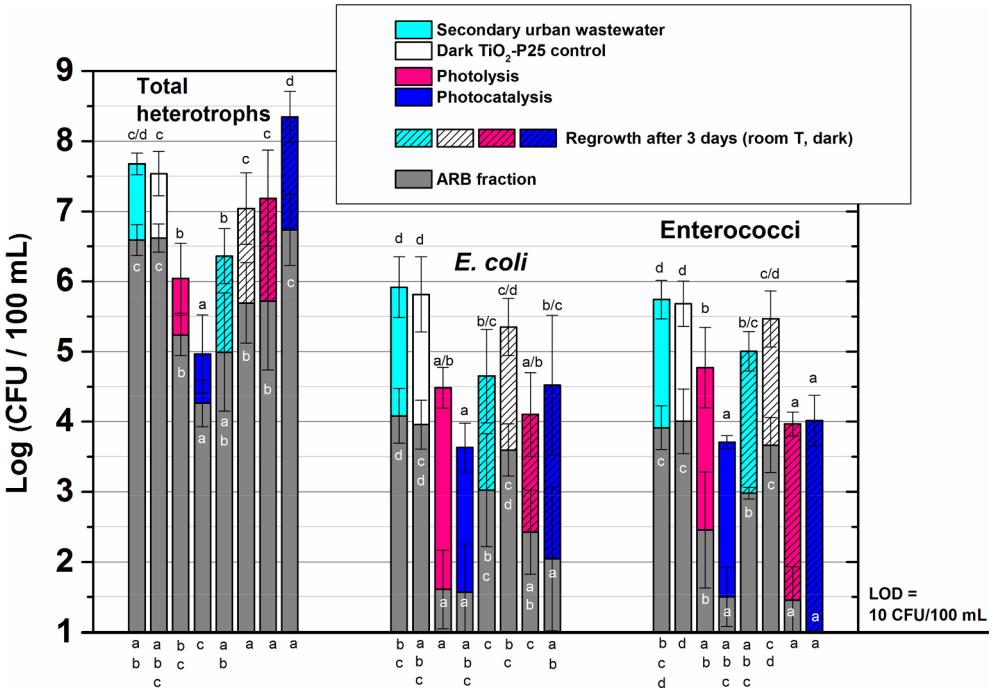

Fig. 6. Total (coloured) and antibiotic resistant (grey) bacteria inactivation after 1 h photolysis/photocatalysis evaluated immediately (filled bars) and after 3-day storage in dark at room temperature (striped bars). The letters a, b, c, d and e indicate significantly ($p < 0.05$) different groups among the tested treatment conditions. The letters in black on the top of bars refer to total bacteria. The letters in white refer to the antibiotic resistant counterparts. The letters on the bottom of the graph refer to the percentage of resistant bacteria with respect to the total bacteria. (For interpretation of the colour references, the reader should refer to the electronic web version of the article).

LEDs. Bacterial inactivation reached values of about 2 log-units, although this apparent removal was not enough to avoid bacterial regrowth of total heterotrophs to values close to those observed before treatment. The prevalence of antibiotic resistance after regrowth was similar (for total heterotrophs and *E. coli*) or lower (for enterococci) than in non-treated UWW, suggesting that resistant bacteria were not more fitted to regrow than their susceptible counterparts. Nevertheless, the microbiological risks associated with these effects in UWW treated by this and other AOPs are still a matter of concern that requires to be assessed. Even so, the results presented suggest the potential of UVA-LEDs photocatalysis to be successfully used as part of the tertiary treatment of UWW. The cost effectiveness in terms of energy consumption per volume of treated UWW, the design of new reactor configurations in what concerns to optimal light distribution, immobilization of the photocatalyst on adequate substrates, and the definition of conditions to minimize microbial regrowth, are critical aspects to consider for a successful implementation.

Acknowledgments

This work is part of a project that has received funding from the European Union's Horizon 2020 research and innovation programme under the Marie Skłodowska-Curie grant agreement No 675530. The content of this publication reflects only the authors' views and the Research Executive Agency is not responsible for any use that may be made of the information it contains. This work was also supported by Projects NORTE-01-0247-FEDER-033330 (DEPCAT) funded by ERDF/FEDER (European Regional Development Fund) through NORTE 2020 (Norte Portugal Regional Operational Programme), Associate Laboratory LSRE-LCM – UID/EQU/50020/2019, and LEPABE – UID/EQU/00511/2019, funded by national funds through FCT/MCTES (PIDDAC). NFFM acknowledges FCT (PD/BD/114318/2016).

Appendix A. Supplementary data

Supplementary data to this article can be found online at https://doi.org/10.1016/j.cej.2019.02.012.

References

[1] I.T. Carvalho, L. Santos, Antibiotics in the aquatic environments: a review of the European scenario, Environ. Int. 94 (2016) 736–757, https://doi.org/10.1016/j.envint.2016.06.025.

[2] M.O. Barbosa, N.F.F. Moreira, A.R. Ribeiro, M.F.R. Pereira, Occurrence and removal of organic micropollutants: an overview of the watch list of EU Decision 2015/495, Water Res. 94 (2016) 257–279, https://doi.org/10.1016/j.watres.2016.02.047.

[3] J.C.G. Sousa, A.R. Ribeiro, M.O. Barbosa, M.F.R. Pereira, A.M.T. Silva, A review on environmental monitoring of water organic pollutants identified by EU guidelines, J. Hazard. Mater. 344 (2018) 146–162, https://doi.org/10.1016/J.JHAZMAT.2017.09.058.

[4] P. Verlicchi, M. Al Aukidy, E. Zambello, Occurrence of pharmaceutical compounds in urban wastewater: removal, mass load and environmental risk after a secondary treatment-A review, Sci. Total Environ. 429 (2012) 123–155, https://doi.org/10.1016/j.scitotenv.2012.04.028.

[5] Directive, COMMISSION IMPLEMENTING DECISION (EU) 2015/495 of 20 March 2015 establishing a watch list of substances for Union-wide monitoring in the field of water policy pursuant to Directive 2008/105/EC of the European Parliament and of the Council, Off. J. Eur. Union. L78 (2015) 40–43. https://eur-lex.europa.eu/legal-content/EN/TXT/PDF/?uri=CELEX:32015D0495&from=EN (accessed July 8, 2018).

[6] Directive, COMMISSION IMPLEMENTING DECISION (EU) 2018/840 of 5 June 2018 establishing a watch list of substances for Union-wide monitoring in the field of water policy pursuant to Directive 2008/105/EC of the European Parliament and of the Council and repealing Comm, Off. J. Eur. Union. L141 (2018) 9–12.

[7] L. Rizzo, C. Manaia, C. Merlin, T. Schwartz, C. Dagot, M.C. Ploy, I. Michael, D. Fatta-Kassinos, Urban wastewater treatment plants as hotspots for antibiotic resistant bacteria and genes spread into the environment: a review, Sci Total Env. 447 (2013) 345–360, https://doi.org/10.1016/j.scitotenv.2013.01.032.

[8] A. Karkman, T.T. Do, F. Walsh, M.P.J. Virta, Antibiotic-resistance genes in waste water, Trends Microbiol. 26 (2018) 220–228, https://doi.org/10.1016/j.tim.2017.09.005.

[9] C.M. Manaia, J. Rocha, N. Scaccia, R. Marano, E. Radu, F. Biancullo, F. Cerqueira, G. Fortunato, I. Iakovides, I. Zammit, I. Kampouris, I. Vaz-Moreira, O.C. Nunes, Antibiotic resistance in wastewater treatment plants: tackling the black box, Environ. Int. 115 (2018) 312–324, https://doi.org/10.1016/j.envint.2018.03.044.

[10] G. Ferro, A. Fiorentino, M.C. Alferez, M.I. Polo-Lòpez, L. Rizzo, P. Fernàndez-Ibànez, Urban wastewater disinfection for agricultural reuse: effect of solar driven AOPs in the inactivation of a multidrug resistant *E. coli* strain, Appl. Catal. B Environ. 178 (2015) 65–73, https://doi.org/10.1016/j.apcatb.2014.10.043.

[11] A. Christou, A. Agüera, J.M. Bayona, E. Cytryn, V. Fotopoulos, C.M. Manaia, C. Michael, M. Revitt, P. Schroder, D. Fatta-Kassinos, The potential implications of reclaimed wastewater reuse for irrigation on the agricultural environment: the knowns and unknowns of the fate of antibiotics and antibiotic resistant bacteria and resistance genes – a review, Water Res. 123 (2017) 448–467, https://doi.org/10.1016/j.watres.2017.07.004.

[12] A. Christou, P. Karaolia, E. Hapeshi, C. Michael, D. Fatta-Kassinos, Long-term wastewater irrigation of vegetables in real agricultural systems: concentration of pharmaceuticals in soil, uptake and bioaccumulation in tomato fruits and human health risk assessment, Water Res. 109 (2017) 24–34, https://doi.org/10.1016/j.watres.2016.11.033.

[13] I. Michael, L. Rizzo, C.S. Mcardell, C.M. Manaia, C. Merlin, T. Schwartz, C. Dagot, D. Fatta-Kassinos, Urban wastewater treatment plants as hotspots for the release of antibiotics in the environment: a review, Water Res. 47 (2012) 957–995, https://doi.org/10.1016/j.watres.2012.11.027.

[14] D. Fatta-Kassinos, M.I. Vasquez, K. Kümmerer, Transformation products of pharmaceuticals in surface waters and wastewater formed during photolysis and advanced oxidation processes – degradation, elucidation of byproducts and assessment of their biological potency, Chemosphere 85 (2011) 693–709, https://doi.org/10.1016/j.chemosphere.2011.06.082.

[15] L. Rizzo, A. Fiorentino, A. Anselmo, Advanced treatment of urban wastewater by UV radiation: effect on antibiotics and antibiotic-resistant *E. coli* strains, Chemosphere 92 (2013) 171–176, https://doi.org/10.1016/j.chemosphere.2013.03.021.

[16] J.M. Sousa, M. Pedrosa, C. Becerra-Castro, S. Castro-Silva, M.F.R. Pereira, A.M.T. Silva, O.C. Nunes, C.M. Manaia, Ozonation and UV_{254} nm radiation for the removal of microorganisms and antibiotic resistance genes from urban wastewater, J. Hazard. Mater. 323 (2017) 434–441, https://doi.org/10.1016/j.jhazmat.2016.03.096.

[17] C. Becerra-Castro, G. Macedo, A.M.T. Silva, C.M. Manaia, O.C. Nunes, Proteobacteria become predominant during regrowth after water disinfection, Sci. Total Environ. 573 (2016) 313–323, https://doi.org/10.1016/j.scitotenv.2016.08.054.

[18] H.Y. Kim, T.-H. Kim, S. Yu, Photolytic degradation of sulfamethoxazole and trimethoprim using UV-A, UV-C and vacuum-UV (VUV), J. Environ. Sci. Heal. Part A. 50 (2015) 292–300, https://doi.org/10.1080/10934529.2015.981118.

[19] M.N. Abellàn, J. Giménez, S. Esplugas, Photocatalytic degradation of antibiotics: The case of sulfamethoxazole and trimethoprim, Catal. Today 144 (2009) 131–136, https://doi.org/10.1016/j.cattod.2009.01.051.

[20] P. Xiong, J. Hu, Decomposition of acetaminophen (Ace) using TiO_2/UVA/LED system, Catal. Today 282 (2017) 48–56, https://doi.org/10.1016/j.cattod.2016.03.015.

[21] P. Xiong, J. Hu, Inactivation/reactivation of antibiotic-resistant bacteria by a novel UVA/LED/TiO_2 system, Water Res. 47 (2013) 4547–4555, https://doi.org/10.1016/J.WATRES.2013.04.056.

[22] N.F.F. Moreira, J.M. Sousa, G. Macedo, A.R. Ribeiro, L. Barreiros, M. Pedrosa, J.L. Faria, M.F.R. Pereira, S. Castro-Silva, M.A. Segundo, C.M. Manaia, O.C. Nunes, A.M.T. Silva, Photocatalytic ozonation of urban wastewater and surface water using immobilized TiO_2 with LEDs: Micropollutants, antibiotic resistance genes and estrogenic activity, Water Res. 94 (2016) 10–22, https://doi.org/10.1016/j.watres.2016.02.003.

[23] Q. Cai, J. Hu, Decomposition of sulfamethoxazole and trimethoprim by continuous UVA/LED/TiO_2 photocatalysis: decomposition pathways, residual antibacterial activity and toxicity, J. Hazard. Mater. 323 (2017) 527–536, https://doi.org/10.1016/j.jhazmat.2016.06.006.

[24] N. Jallouli, L.M. Pastrana-Martínez, A.R. Ribeiro, N.F.F. Moreira, J.L. Faria, O. Hentati, A.M.T. Silva, M. Ksibi, Heterogeneous photocatalytic degradation of ibuprofen in ultrapure water, municipal and pharmaceutical industry wastewaters using a TiO_2/UV-LED system, Chem. Eng. J. 334 (2018) 976–984, https://doi.org/10.1016/j.cej.2017.10.045.

[25] M.J. Arlos, R. Liang, L.C.M. Li, C. Fong, N.Y. Zhou, C.J. Ptacek, S.A. Andrews, M.R. Servos, Influence of methanol when used as a water-miscible carrier of pharmaceuticals in TiO_2 photocatalytic degradation experiments, J. Environ. Chem. Eng. 5 (2017) 4497–4504, https://doi.org/10.1016/j.jece.2017.08.048.

[26] L.C. Ferreira, M.S. Lucas, J.R. Fernandes, P.B. Tavares, Photocatalytic oxidation of Reactive Black 5 with UV-A LEDs, J. Environ. Chem. Eng. 4 (2016) 109–114, https://doi.org/10.1016/j.jece.2015.10.042.

[27] G. Matafonova, V. Batoev, Recent advances in application of UV light-emitting diodes for degrading organic pollutants in water through advanced oxidation processes: a review, Water Res. 132 (2018) 177–189, https://doi.org/10.1016/j.watres.2017.12.079.

[28] R. van Grieken, J. Marugán, C. Pablos, L. Furones, A. López, Comparison between the photocatalytic inactivation of Gram-positive *E. faecalis* and Gram-negative *E. coli* faecal contamination indicator microorganisms, Appl. Catal. B Environ. 100 (2010) 212–220, https://doi.org/10.1016/j.apcatb.2010.07.034.

[29] J. Marugán, R. Van Grieken, C. Pablos, M.L. Satuf, A.E. Cassano, O.M. Alfano, Rigorous kinetic modelling with explicit radiation absorption effects of the photocatalytic inactivation of bacteria in water using suspended titanium dioxide, Appl. Catal. B Environ. 102 (2011) 404–416, https://doi.org/10.1016/j.apcatb.2010.12.012.

[30] L. Rizzo, A. Della Sala, A. Fiorentino, G. Li Puma, Disinfection of urban wastewater by solar driven and UV lamp – TiO_2 photocatalysis: Effect on a multi drug resistant *Escherichia coli* strain, Water Res. 53 (2014) 145–152, https://doi.org/10.1016/j.watres.2014.01.020.
[31] M. Martín-Sómer, C. Pablos, R. van Grieken, J. Marugán, Influence of light distribution on the performance of photocatalytic reactors: LED vs mercury lamps, Appl. Catal. B Environ. 215 (2017) 1–7, https://doi.org/10.1016/j.apcatb.2017.05.048.
[32] M.L. Satuf, R.J. Brandi, A.E. Cassano, O.M. Alfano, Experimental method to evaluate the optical properties of aqueous titanium dioxide suspensions, Ind. Eng. Chem. Res. 44 (2005) 6643–6649, https://doi.org/10.1021/ie050365y.
[33] G. Li Puma, A. Brucato, Dimensionless analysis of slurry photocatalytic reactors using two-flux and six-flux radiation absorption-scattering models, Catal. Today 122 (2007) 78–90, https://doi.org/10.1016/j.cattod.2007.01.027.
[34] A.R. Ribeiro, M. Pedrosa, N.F.F. Moreira, M.F.R. Pereira, A.M.T. Silva, Environmental friendly method for urban wastewater monitoring of micropollutants defined in the Directive 2013/39/EU and Decision 2015/495/EU, J. Chromatogr. A. 1418 (2015) 140–149, https://doi.org/10.1016/j.chroma.2015.09.057.
[35] A. Novo, S. Andre, P. Viana, O.C. Nunes, M. Manaia, Antibiotic resistance, antimicrobial residues and bacterial community composition in urban wastewater, Water Res. 47 (2013) 1875–1887, https://doi.org/10.1016/j.watres.2013.01.010.
[36] CLSI, M100S Performance Standards for Antimicrobial, Susceptibility Testing (2016).
[37] D. Vione, J. Feitosa-Felizzola, C. Minero, S. Chiron, Phototransformation of selected human-used macrolides in surface water: kinetics, model predictions and degradation pathways, Water Res. 43 (2009) 1959–1967, https://doi.org/10.1016/j.watres.2009.01.027.
[38] S. Hanamoto, N. Nakada, N. Yamashita, H. Tanaka, Modeling the photochemical attenuation of down-the-drain chemicals during river transport by stochastic methods and field measurements of pharmaceuticals and personal care products, Environ. Sci. Technol. 47 (2013) 13571–13577, https://doi.org/10.1021/es4035478.
[39] L. Ge, J. Chen, X. Wei, S. Zhang, X. Qiao, X. Cai, Q. Xie, Aquatic photochemistry of fluoroquinolone antibiotics: kinetics, pathways, and multivariate effects of main water constituents, Environ. Sci. Technol. 44 (2010) 2400–2405, https://doi.org/10.1021/es902852v.
[40] K.H. Wammer, A.R. Korte, R.A. Lundeen, J.E. Sundberg, K. Mcneill, W.A. Arnold, Direct photochemistry of three fluoroquinolone antibacterials: norfloxacin, ofloxacin, and enrofloxacin, Water Res. 47 (2013) 439–448, https://doi.org/10.1016/j.watres.2012.10.025.
[41] C.C. Ryan, D.T. Tan, W.A. Arnold, Direct and indirect photolysis of sulfamethoxazole and trimethoprim in wastewater treatment plant effluent, Water Res. 45 (2010) 1280–1286, https://doi.org/10.1016/j.watres.2010.10.005.
[42] S. Yan, B. Yao, L. Lian, X. Lu, S.A. Snyder, R. Li, W. Song, Development of fluorescence surrogates to predict the photochemical transformation of pharmaceuticals in wastewater effluents, Environ. Sci. Technol. 51 (2017) 2738–2747, https://doi.org/10.1021/acs.est.6b05251.
[43] L. Tong, P. Eichhorn, S. Pérez, Y. Wang, D. Barceló, Photodegradation of azithromycin in various aqueous systems under simulated and natural solar radiation: Kinetics and identification of photoproducts, Chemosphere 83 (2011) 340–348, https://doi.org/10.1016/j.chemosphere.2010.12.025.
[44] E. Hapeshi, A. Achilleos, M.I. Vasquez, C. Michael, N.P. Xekoukoulotakis, D. Mantzavinos, D. Kassinos, Drugs degrading photocatalytically: kinetics and mechanisms of ofloxacin and atenolol removal on titania suspensions, Water Res. 44 (2010) 1737–1746, https://doi.org/10.1016/j.watres.2009.11.044.
[45] S. Malato, P. Fernández-Ibáñez, M.I. Maldonado, J. Blanco, W. Gernjak, Decontamination and disinfection of water by solar photocatalysis: recent overview and trends, Catal. Today 147 (2009) 1–59, https://doi.org/10.1016/J.CATTOD.2009.06.018.
[46] J. Herrmann, Heterogeneous photocatalysis: fundamentals and applications to the removal of various types of aqueous pollutants, Catal. Today 53 (1999) 115–129, https://doi.org/10.1016/S0920-5861(99)00107-8.
[47] N.F.F. Moreira, C.A. Orge, A.R. Ribeiro, J.L. Faria, O.C. Nunes, M.F.R. Pereira, A.M.T. Silva, Fast mineralization and detoxification of amoxicillin and diclofenac by photocatalytic ozonation and application to an urban wastewater, Water Res. 87 (2015) 87–96, https://doi.org/10.1016/j.watres.2015.08.059.
[48] L. Prieto-Rodriguez, S. Miralles-Cuevas, I. Oller, A. Agüera, G.L. Puma, S. Malato, Treatment of emerging contaminants in wastewater treatment plants (WWTP) effluents by solar photocatalysis using low TiO_2 concentrations, J. Hazard. Mater. 211–212 (2012) 131–137, https://doi.org/10.1016/j.jhazmat.2011.09.008.
[49] I. Kim, N. Yamashita, H. Tanaka, Performance of UV and UV/H_2O_2 processes for the removal of pharmaceuticals detected in secondary effluent of a sewage treatment plant in Japan, J. Hazard. Mater. 166 (2009) 1134–1140, https://doi.org/10.1016/j.jhazmat.2008.12.020.
[50] J. Alexander, G. Knopp, A. Dötsch, A. Wieland, T. Schwartz, Ozone treatment of conditioned wastewater selects antibiotic resistance genes, opportunistic bacteria, and induce strong population shifts, Sci. Total Environ. 559 (2016) 103–112, https://doi.org/10.1016/j.scitotenv.2016.03.154.
[51] G. Ferro, F. Guarino, S. Castiglione, L. Rizzo, Antibiotic resistance spread potential in urban wastewater effluents disinfected by UV/H_2O_2 process, Sci. Total Environ. 560–561 (2016) 29–35, https://doi.org/10.1016/j.scitotenv.2016.04.047.
[52] P.S.M. Dunlop, M. Ciavola, L. Rizzo, D.A. Mcdowell, J.A. Byrne, Effect of photocatalysis on the transfer of antibiotic resistance genes in urban wastewater, Catal. Today 240 (2015) 55–60, https://doi.org/10.1016/j.cattod.2014.03.049.
[53] I. Michael-Kordatou, P. Karaolia, D. Fatta-Kassinos, The role of operating parameters and oxidative damage mechanisms of Advanced Chemical Oxidation Processes in the combat against antibiotic-resistant bacteria and resistance genes present in urban wastewater, Water Res. 129 (2018) 208–230, https://doi.org/10.1016/J.WATRES.2017.10.007.
[54] M. Guo, Q. Yuan, J. Yang, Microbial selectivity of UV treatment on antibiotic-resistant heterotrophic bacteria in secondary effluents of a municipal wastewater treatment plant, Water Res. 47 (2013) 6388–6394, https://doi.org/10.1016/j.watres.2013.08.012.
[55] A.M. Ibekwe, S.E. Murinda, C. DebRoy, G.B. Reddy, Potential pathogens, antimicrobial patterns and genotypic diversity of *Escherichia coli* isolates in constructed wetlands treating swine wastewater, FEMS Microbiol. Ecol. 92 (2016) 1–14, https://doi.org/10.1093/femsec/fiw006.
[56] I. Michael, E. Hapeshi, C. Michael, A.R. Varela, S. Kyriakou, C.M. Manaia, D. Fatta-Kassinos, Solar photo-Fenton process on the abatement of antibiotics at a pilot scale: degradation kinetics, ecotoxicity and phytotoxicity assessment and removal of antibiotic resistant enterococci, Water Res. 46 (2012) 5621–5634, https://doi.org/10.1016/j.watres.2012.07.049.
[57] P. Karaolia, I. Michael-Kordatou, E. Hapeshi, C. Drosou, Y. Bertakis, D. Christofilos, G.S. Armatas, L. Sygellou, T. Schwartz, N.P. Xekoukoulotakis, D. Fatta-Kassinos, Removal of antibiotics, antibiotic-resistant bacteria and their associated genes by graphene-based TiO_2 composite photocatalysts under solar radiation in urban wastewaters, Appl. Catal. B Environ. 224 (2018) 810–824, https://doi.org/10.1016/j.apcatb.2017.11.020.
[58] X. Zhao, H.-Y. Hu, T. Yu, C. Su, H. Jiang, S. Liu, Effect of different molecular weight organic components on the increase of microbial growth potential of secondary effluent by ozonation, J. Environ. Sci. 26 (2014) 2190–2197, https://doi.org/10.1016/J.JES.2014.09.001.
[59] N.F.F. Moreira, C. Narciso-da-Rocha, M. Inmaculada Polo-López, L.M. Pastrana-Martínez, J.L. Faria, C.M. Manaia, P. Fernández-Ibáñez, O.C. Nunes, A.M.T. Silva, Solar treatment (H_2O_2, TiO_2-P25 and GO-TiO_2 photocatalysis, photo-Fenton) of organic micropollutants, human pathogen indicators, antibiotic resistant bacteria and related genes in urban wastewater, Water Res. 135 (2018) 195–206, https://doi.org/10.1016/j.mechrescom.2007.09.002.
[60] A. Fiorentino, G. Ferro, M.C. Alferez, M.I. Polo-López, P. Fernández-Ibañez, L. Rizzo, Inactivation and regrowth of multidrug resistant bacteria in urban wastewater after disinfection by solar-driven and chlorination processes, J. Photochem. Photobiol. B Biol. 148 (2015) 43–50, https://doi.org/10.1016/j.jphotobiol.2015.03.029.
[61] P. Thayanukul, F. Kurisu, I. Kasuga, H. Furumai, Evaluation of microbial regrowth potential by assimilable organic carbon in various reclaimed water and distribution systems, Water Res. 47 (2013) 225–232, https://doi.org/10.1016/J.WATRES.2012.09.051.
[62] P.V. Laxma Reddy, B. Kavitha, P.A. Kumar Reddy, K.-H. Kim, TiO_2-based photocatalytic disinfection of microbes in aqueous media: A review, Environ. Res. 154 (2017) 296–303, https://doi.org/10.1016/J.ENVRES.2017.01.018.